https://ntrs.nasa.gov/search.jsp?R=19830015441 2020-03-21T04:39:56+00:00Z

General Disclaimer

One or more of the Following Statements may affect this Document

- This document has been reproduced from the best copy furnished by the organizational source. It is being released in the interest of making available as much information as possible.

- This document may contain data, which exceeds the sheet parameters. It was furnished in this condition by the organizational source and is the best copy available.

- This document may contain tone-on-tone or color graphs, charts and/or pictures, which have been reproduced in black and white.

- This document is paginated as submitted by the original source.

- Portions of this document are not fully legible due to the historical nature of some of the material. However, it is the best reproduction available from the original submission.

Produced by the NASA Center for Aerospace Information (CASI)

DOE/JPL-956053-82/4
9950-788

University of Illinois at Chicago

College of Engineering
DEPARTMENT OF CIVIL ENGINEERING,
MECHANICS, AND METALLURGY

Post Office Box 4348
Chicago, Illinois 60680
(312) 996-3428

STUDY OF ABRASIVE WEAR RATE OF SILICON USING n-ALCOHOLS

by

Steven Danyluk
University of Illinois at Chicago
Department of Civil Engineering, Mechanics and Metallurgy
Chicago, Illinois 60680

Sponsored by

The U.S. Department of Energy/Jet Propulsion Laboratory
Flat-Plate Solar Array Project
Contract No. 956053

(NASA-CR-170242) STUDY OF ABRASIVE WEAR RATE OF SILICON USING n-ALCOHOLS Quarterly Progress Report (Illinois Univ.) 50 p HC A03/MF A01 CSCL 10A

N83-23712

Unclas G3/44 09906

APR 1983
RECEIVED
NASA STI FACILITY
ACCESS DEPT.

This work comprises results obtained by J. Clark, S. W. Lee and D. S. Lim, graduate students in the Civil Engineering, Mechanics and Metallurgy Department at the University of Illinois at Chicago.

Report No. 82-1

Fourth Quarterly Progress Report
to the

U.S. Department of Energy/Jet Propulsion Laboratory
Flat-Plate Solar Array Project

for the period

April 16, 1982 - July 15, 1982

Contract No. 956053

STUDY OF ABRASIVE WEAR RATE OF SILICON USING n-ALCOHOLS

by

Steven Danyluk

STUDY OF ABRASIVE WEAR RATE OF SILICON USING n-ALCOHOLS

by

Steven Danyluk
Department of Civil Engineering, Mechanics and Metallurgy
University of Illinois at Chicago
Chicago, Illinois 60680

ABSTRACT

This quarterly report summarizes the work carried out at the University of Illinois at Chicago for the Flat-Plate Solar Array Project under contract No. 956053. The main emphasis of this work has been a determination of the abrasion wear rate of silicon in a number of fluid environments and a determination of the parameters that influence the surface mechanical properties of silicon. Three tests were carried out in this study: circular and linear multiple-scratch test, microhardness test and a three-point bend test. These test methods have allowed a sorting of the pertinent parameters such as: effect of surface orientation, dopant and fluid properties. A brief review and critique of previous work is presented.

ACKNOWLEDGEMENTS

This work is supported by the U.S. Department of Energy/Jet Propulsion Laboratory Solar Array Project under Contract No. 956053 with S. Danyluk as the principal investigator. This support is gratefully acknowledged. Thanks are due to K. Koliwad and J. Liu for encouragement at the early stages of this work, S. Hyland and C. P. Chen for technical discussions and T. Daud and M. Leipold for continued interest. The silicon wafers used in this study were provided by S. Hyland of JPL and J. Farber of Monsanto. Special thanks go to M. Naegele and C. Scott for technical assistance.

TABLE OF CONTENTS

1. INTRODUCTION

Abrasive cutting and polishing are used extensively in the semiconductor and glass industries for processing large scale integrated circuits and producing appropriate finishes on surfaces. These techniques involve the use of abrasive particles usually suspended in a fluid and the motion of these particles relative to the surface of the semiconductor or glass. Silicon, germanium and III-V semiconductor compounds, for example, are processed by cutting and polishing in a slurry of SiC, Al_2O_3 or diamond. In the solar photovoltaic industry [1], silicon is cut into sheet by (a) inner diameter saw wafering, (b) multiblade wafering using a slurry and (c) multiwire wafering using a fixed abrasive and a slurry. These methods rely on abrasive wear for cutting by the motion of diamond-impregnated wires, abrasive wheels or silicon carbide slurries in water or an oil-based carrier. The abrasives slide across the surface and form grooves as the material is removed in the form of microchips. If the abrasive particles are loose then they may move relative to one another and possibly rotate while sliding across the wearing surface [2]. Whether the abrasive is fixed or loose, a high material removal rate and a minimum in near surface damage is desired. In the cases described above, the interaction of the fluid with the abrasive particle and the abrading surface can have a profound influence on the wear rate and the near surface damage of the abrading surface.

Fluids can have a significant influence on the surface mechanical properties of non-metals. These effects were first reported by Rehbinder [3] and a clearer understanding has been contributed by Westwood and others [4]. It has been proposed by Westwood that adsorption of polar molecules can alter the near-surface point defect and dislocation distribution and, consequently, the interactions of these defects can be affected. If the near-surface

ORIGINAL PAGE IS
OF POOR QUALITY

dislocation mobility is affected, for example, by kink generation, then the surface mechanical properties such as hardness and as a consequence the abrasive wear are altered. Although these effects are now well documented in oxides and glasses, the relation of fluid interaction to the abrasive wear of semiconductors has not been investigated to the same extent [5].

Ongoing research conducted at the University of Illinois at Chicago under a grant from the Jet Propulsion Laboratory, Flat-Plate Solar Array Project (Contract No. 956053) for this past year has shown that different fluids can effect to a significant extent the wear rate of diamond abrading silicon--a factor of two difference in wear rate can be obtained, for example, between absolute ethanol and de-ionized water. In addition, the depth of damage below the abraded surface is also influenced by the fluid used in the abrasion process.

Three earlier quarterly reports briefly summarized the initial stages of this research and the magnitudes of the effects observed [4]. This report summarizes the work performed in the final quarter of the first year and puts in perspective the scope of the work and the direction of the work for the coming year.

A brief review of the present state of abrasive wear of silicon and the influence of fluids on the surface mechanical properties of silicon is presented. The experiments that were performed are listed in separate sections along with the results and our view of the significance of the results. In each case, where possible, the results are described in terms of a model of the deformation of silicon.

OF POOR

2. BACKGROUND

Comprehensive surveys of the present state of knowledge of the effects of fluids on the surface mechanical properties of non-metals have recently been published [5] and will not be reviewed here. We will summarize only those parts of previous studies that deal with semiconductors and the influence of light, fluid and voltage on the surface mechanical properties of semiconductors.

2.1 Influence of Light, Fluid and Voltage on the Surface Mechanical Properties of Silicon

The surface mechanical properties of silicon can be modified either by light (photo-mechanical effect), fluids (chemo-mechanical effect) or electrostatic potential. A modification of the surface hardness of silicon was first reported by Kuczynski and Hochman [6]. A softened layer (70% softening) of one to two microns as determined by Knoop indentations when 2.0-4.0 μm wavelength light was shone on the surface and was proportional to light intensity and influenced by surface preparation. The effect was interpreted in terms of energy states of dislocations and space charge layers in the silicon. The infrared and ultraviolet light was thought to alter the energy of the dislocations in the space charge region and thereby affect the plastic properties.

Ablow [7] investigated the microhardness of silicon as a function of surface preparation, humidity and impurity content. A softening of the surface was also observed and depended on the level of impurity concentration and ambient H_2O. The affect was described in terms of space charge layers and interaction with charged dislocations formed in the deformation process. It was not explained how the ambient environment affected the surface softening.

ORIGINAL PAGE IS
OF POOR QUALITY

Westbrook and Gilman [8] found that a softening (up to 60%) occurred in silicon (2-3 μm deep) when indentations were carried out in the presence of a small potential (0.05 - 10 v) between the indenter and the crystal surface. The effect disappeared at elevated temperatures and was not sensitive to the type of charge carrier. A model or mechanism was not proposed.

The effects of fluid environments were examined by Yost and Williams [9] who reported on a minimum in hardness for n- and p-type silicon with concentration in NaCl and $Na_4P_2O_7$ for a maximum in the negative zeta potential. These results indicated that the hardness change with zeta potential is related to the surface charge and the influence on the charge carrier concentration at the surface. The surface charges are thought to interact with charged kinks at dislocations. The zeta potentials were obtained after crushing the silicon on which hardness tests were performed. Since crushing has been shown to induce surface states [10] which would modify the space charge regions and surface potentials, the validity of the above results can be questioned.

Recently Cuthrell [11] reported that the deformation mode during drilling silicon in the presence of CCl_4 and H_2O changed from ductile ploughing to brittle fracture, respectively. The affect was speculated to be due to hydrogen embrittlement.

Chen and Knapp [12] reported no time-dependent fracture of silicon when a Knoop indentation was used to create a flaw and the sample stressed was in contact with water, salt water, dilute solutions of NH_4OH and HNO_3 and acetone. These results were interpreted to mean that static loads do not influence the deformation behavior of silicon.

Kuan, Shih, Van Vechten and Westdorp [13] examined the effect of lubricants on the structure of the surface damage induced in silicon during the wafering process. Water, methyl silane, kleenzol B and dielectric oil were used and the damage (surface cracks) was investigated by transmission

electron microscopy. The depth of the saw damage was lower for kleenzol B and methyl silane as compared with dielectric oil. A positive potential on the silicon increased the depth of the damage and decreased it for a negative potential. These effects were interpreted as lubricant dampening the out-of-plane blade vibration which results in less surface damage.

The above discussion is summarized in Table I which shows the changes in surface hardness of silicon. As can be seen, a softening of up to 80% has been reported, depending on the external variables and type of experiment used in the study.

The above results on silicon have been interpreted in terms of the chemo-mechanical model proposed by Westwood.

Westwood, et al. [18,19] proposed that chemisorbed molecules influence the mobility of near surface dislocations of non-metals and suggested that chemisorption induced variations in the electron occupancy of dislocation core states can influence the nucleation rate of dislocation kinks near the surface. The magnitude of the chemisorption should influence the space charge region and therefore a change in the Debye length should be reflected in the surface mechanical properties. The Debye length is directly proportional to the dielectric constant and inversely proportional to the charged-ion concentration and temperature of the fluid. Indeed a correlation was found by Cuthrell [20] in drilling experiments of Pyrex glass between acoustic emission signals and dielectric constants. The model is linked to dissociated ion production in solutions of high dielectric constant ($\varepsilon > 40$), ion pairs formed between $20 < \varepsilon < 40$ and triplets formed below $\varepsilon \sim 20$. A determination of abrasion rate vs. dielectric constant of fluids and temperature should confirm the chemisorption-space change model.

In addition, since the adsorption is linked to dislocation density in the surface region, the number of chemisorption sites which would have different binding energies from ledge or kink sites should be limited and the filling of these sites should depend on temperature. An analogous model was successfully employed to explain experimental results of halide ion adsorption on the silver halide surfaces [21,22].

3. EXPERIMENTAL PROGRAM

The primary objective of this investigation is to study the influence of fluids on the surface mechanical properties of silicon. This objective is carried out by performing abrasion experiments that simulate the presently used cutting technologies in other programs of the Flat-Plate Solar Array Project but with the emphasis being on the fundamental mechanisms of wear. Subsidiary experiments were also carried out on the microhardness of (100) and (111) n- and p-type silicon in the presence of fluids and, the depth of damage that results during the abrasion in fluids. The fracture of abraded silicon wafers has also been initiated and these plans are detailed in this section.

3.1 Parameters to be Investigated

A flowchart of the experimental program and the expected results are shown in Fig. 1. This past year, all three aspects of the experimental program were carried out and we will report on the progress of this work. The initial emphasis of this work was on the abrasion and wear testing of silicon and

consequently the bulk of this report will comprise results from this part of the program.

3.2 Abrasive Wear Testing of Silicon and Germanium

The experimental apparatus used in this part of the study was designed to simulate the cutting technologies used for the processing of silicon. A schematic of the experiment is shown in Fig. 2 as previously reported [14]. This apparatus is similar to the pin-on-disk design used in abrasive wear testing except that the abrasive particle is a single crystal pyramid diamond and the silicon rotates past the diamond, and a multi-scratch groove is formed. The diamond is held against the silicon by dead-weight loading as the silicon is rotated at a fixed speed. The diamond is prevented from lateral motion and a groove is formed, the depth of which depends on the time allowed for abrasion. A series of grooves are generated by varying the time of rotation. During the rotation of the silicon a fluid is introduced and completely covers the silicon surface. Only one fluid per silicon wafer is used. In addition, the dead load force, F_N, and the speed of rotation, ω, can also be varied.

Prior to abrasion, the surfaces were cleaned in the following way. The silicon and germanium are prepared by dipping in a 10 v/o hydrofloric acid (HF) bath for 30 s, rinsing in de-ionized water and drying, then immediately immersing in the fluid for testing. The silicon wafers have previously been lapped, polished and etched according to semiconductor industry standards.

Representative micrographs of the surfaces of the silicon wafers abraded in the presence of de-ionized water, 5 w/o NaCl + de-ionized water, acetone and ethanol are shown in Fig. 3. The normal force was 0.098 N and the

abrading time was 1.8×10^3 s, all other variables being held constant. As can be seen, the groove surface morphology changes when the fluid is changed, similar to the results previously reported [14]. Conchoidal fracture of the side walls near the top surface is also seen and thus is a result of lateral cracks propagating in the plane of the silicon surface. Micrographs showing this fracture are shown in Fig. 4. Here is shown a terraced structure with the terrace steps containing subsidiary cracks and having a morphology of "river patterns." In this case it appears that the crack initiated at the top surface and propagated toward the groove bottom. Also is shown an unusually large debris particle whose surface replicates the terrace steps. This particle has fractured in a brittle way--very little plasticity is seen. The cross-sectional area of the groove versus abrading time for the four fluids is shown in Figs. 5 and 6. The steady-state rate is represented by the best-fit straight lines. The depth of the groove increases as a function of time and the rate, represented by the slope of the lines, is greatest for ethanol. As expected, as the normal force is decreased, the abraded area is smaller, and just as significantly the slopes of the lines decreases.

As seen in Figs. 5 and 6, the groove depth versus abrading time is significantly influenced by the fluid in contact with the silicon surface. In addition, the mechanism of material removal appears to be influenced by the fluid. We have compared these experimental results with two models; one by Rabinowicz and co-workers [8] who derived a relationship for abrasive wear by a rigid conical asperity carrying a load F_N sliding through a distance S for a single scratch. The expression relating the volume V of material removed to the material hardness H and the geometry of the cone is

ORIGINAL PAGE IS
OF POOR QUALITY

$$V = \frac{F_N S \tan\theta}{\pi H}$$

where θ is the slope angle of the cone measured from the plane of the surface. This equation also applies for the circular multiple-scratch case if it is assumed that for each circumferential distance S_i a volume V_i is removed. The total volume is found by summing S_i and V_i. Substituting $S = t(\omega r)$, $V = 2\pi rA$, $\omega = 0.56$ rev s^{-1}, $\theta = 35°$ and $F_N = 10$ gf for this case (where t is the abrading time, r is the radius of the abrading groove and A is the projected area of the penetrating cone in the vertical plane), the area can be expressed as

$$A = \frac{\tan\theta\, \omega F_N}{2\pi^2 H} \cdot t \qquad (1)$$

The slope of the experimentally determined Area vs. t curve can be compared to the above equation.

The second model is by Evans [9]. The abraded volume removal rate $\dot{V}$ is related to the fracture toughness K_{I_c} and hardness H by the equation

$$V = \frac{0.58\ \psi}{(\pi\beta)^{7/6}} \cdot \frac{F_N^{7/6}}{K_{I_c}^{2/3}\, H^{1/2}} \cdot \ell \qquad (2)$$

where ℓ is the sliding distance, F_N the normal force, ψ a constant ≈ 1 and $\beta = 2/\pi$ for a Vicker's pyramid diamond. Again this equation for the single-scratch test is identical to the multiple-scratch case when all the V_i are summed over the total path length $\ell = 2\pi r\omega$.

The cross-sectional area can be obtained from the above Eq. (2) by substituting $\dot{V} = 2\pi rA/t$ and $\ell = 2\pi r\omega$ so that

$$A = \frac{0.58\ \psi}{(\pi\beta)^{7/6}} \cdot \frac{F_N^{7/6} \cdot \omega}{K_{I_c}^{2/3}\, H^{1/2}} \cdot t \qquad (3)$$

where $\omega = 0.56$ rev s^{-1} and $K_{I_c} = 0.95$ MN/$m^{3/2}$ for (100) fracture surfaces [11] and H is the hardness value obtained for a Vicker's pyramid hardness indenter in the appropriate fluid. The hardness values of the silicon in the appropriate fluid were obtained using a Vickers hardness tester with a 15 gf load on the indenting diamond for 15 s. The hardness values were: 2.0, 2.1, 1.65 and 1.3×10^{10} Nm^{-2} for de-ionized water, the 5 w/o NaCl solution, acetone and ethanol, respectively. These values of H are used to determine dA/dt from Eqs. (1) and (3). The slopes of dA/dt for the Evans and Rabinowicz models and our experimental results from Fig. 5 are shown in Table II. Our data is not well represented by either the Evans model which assumes a lateral crack mechanism for material removal nor the Rabinowicz model. The main difference between the models is that the Rabinowicz model was derived without allowing for plasticity beneath the abraded groove while the Evans model does account for a plastic zone beneath the abraded groove. Our data for the de-ionized water, 5 w/o NaCl + de-ionized water and acetone grooves are consistent with the Rabinowicz brittle model although the differences in rate for these fluids are not well described by this model. The Evans model gives a value significantly higher than the Rabinowicz model and our data for ethanol are also significantly higher as compared with the other three fluids. Although the Evans model in its present form does not describe well the data for ethanol, we believe that the SEM micrographs indicate trends that are consistent with the assumptions in the models. The surfaces abraded in the presence of ethanol show a greater plasticity than the surfaces abraded in the presence of other fluids and as a consequence the abrasion rate in ethanol is higher.

The effect of fluids on the surface mechanical properties of non-metals have been studied by a number of workers. When adsorption of fluids is involved, the effects are called chemo-mechanical effects. A recent summary of the assumptions in this mechanism can be found in the Noordhoff-Leiden Conference [12]. The mechanism for the chemo-mechanical effect involves the adsorption and interaction of the polar fluid with dislocation cores intersecting the surface. The fields due to adsorption can modify the state of charge of the dislocations. Electronic conduction can occur through the electronic states in the band gap that are associated with dangling bonds. Adsorption can therefore pin dislocations and the surface appears harder and more abrasive resistant. When surface plasticity is low as in the case of the de-ionized water, 5 w/o NaCl + de-ionized water and acetone, then the fracture properties dominate the abrasion mechanism and the stress or size effects are dominant. The failure criterion is reached before that for yield. Adsorption to dislocation cores will influence both of these criteria. If the adsorption energy is high then dislocations are pinned and fracture dominates; if adsorption energy is low then dislocations can break free of the pinning sites and the material yields by dislocation motion. Since all the experimental conditions remain constant and only the fluid is changed, the wear results are interpreted in terms of adsorption of the fluid. The adsorption energy of the ethanol should be low compared with the other three fluids. One can judge the adsorption energies by looking at the dielectric constant. The dielectric constant for water, acetone and ethanol are: 79, 21 and 24, respectively. These results may be rationalized by appealing to the argument stated by Cuthrell [13] that adsorption is dominated by a minimum concentration of charged species and a maximum of non-charged species. Our results are consistent with his analysis.

Our results also show that the abrasion rate changes when the normal force changes. For greater loads it was expected that the penetration would be reduced as when boundary lubrication is active. We see just the opposite effect. At light loads the abrasion rate is reduced in addition to the stress effect which lowers the overall curve. Hydrodynamic effects are not considered to have a strong influence at these speeds. The relative magnitudes of hydrodynamic lubrication should scale with the viscosities since all other experimental conditions are held constant. The viscosities at 20°C for water, acetone and ethanol are: 1.002, 1.305 and 1.200 cP [14]. Our wear rates do not scale in this way. The wear in ethanol is twice that for water and acetone. However, the friction coefficient should scale as the Debye length for the adsorbed fluid since friction results from Debye layer interactions [15]. We are not yet able to correlate our wear results with the friction coefficient. Our expectation is that if the fluid is changed but the viscosity remains essentially constant, then this would strongly support the chemo-mechanical mechanism for abrasion of silicon. In our case, the viscosity of the ethanol and acetone are essentially the same but the wear rate is different. We take this to indicate that lubrication in this case is overwhelmed by the chemo-mechanical effect.

In summary, we interpret our results as being consistent with the chemo-mechanical model of dislocation pinning by adsorbed polar molecules. The wear correlates with dielectric properties and not the viscosities of the fluids. We interpret this to mean that chemo-mechanical effects dominate lubrication in this case.

3.3 Depth of Damage Studies in Silicon

The depth of damage of abraded silicon wafers was investigated by a metallographic taper sectioning method. After a groove is made, the wafer is divided to proper dimensions and fixed on a 5° bevel jig using wax. To secure and protect the specimen, two other sliced wafers are attached at the bottom and top of the specimen and a thin layer of wax was used as a coating to prevent the sharp edges from chipping. Manual lapping was done in a horizontal line away from the abrasive emery paper (40 μm SiC). After lapping to 600 grit emery paper the jig was cleaned for 3 min. in an ultrasonic bath to remove any SiC particles. A 10 x 10 x 1/4 in. pyrex flat glass was prepared in which fine scratches were made using Al_2O_3 particles of sizes 6 μm, 3 μm and 1 μm. A 1 μm Al_2O_3 particle slurry with 3 parts distilled water and 1 part glycerin was used as a final polish in this step. The sample was lapped manually in one direction until a flat surface was attained to get the 5° angle. Figure 7 shows a schematic of the experimental arrangement. After lapping, the jig was washed in an ultrasonic bath and a final polish performed using NALCO 2350 slurry which consists of 50% SiO_2 (40-70 mμ) colloid diluted 20 times with distilled water.

After polishing, an etchant was used to delineate the scribed region. The etchant consisted of 8 mℓ of 48% HF and a mixture of 2 gm CrO_3 and 8 mℓ distilled water. Immediately after etching (25-30 s) the specimen was rinsed for 5 min. in distilled water and dried.

Measurement of the lapped and etched grooves was done by recording the depth and width of the groove. Photomicrographs of the polished and etched 5° bevel surfaces is shown in Fig. 8. The normal force F_N was 0.05 N. The groove depth varies with abrasion time for the four fluids indicated. Again, ethanol appears to result in the deepest and widest groove. In addition, the length of subsurface cracks seen extending beyond the tips of the grooves

also varies with time and fluid. The area of these grooves versus abrading time is shown in Fig. 9. The data can be represented for convenience by straight lines, the slopes of which represent the abrasion rate. The rate for ethanol is highest while that for 5 w/o NaCl is lowest.

3.4 Microhardness Tests of Silicon in Fluid Environments

Microhardness tests of (111) p-type and (100) n-type silicon were conducted in eight fluid environments. Prior to testing, wafers of (111) p-type and (100) n-type silicon were cleaned by immersing in a 10% hydrofluoric acid wash for 30 secs, rinsing in de-ionized water and then air dried. Microhardness testing was carried out using the Shimadzu Microhardness Tester Type M. (To facilitate ease in manipulating fluid between tests, the sample anvil and clamp were removed.) A 10 mm by 9 mm region of the sample's polished surface was focused and examined for testing with the 40 x objective. With a micropipet, fluid was applied to form a large drop between the indenter and testing surface. Testing in acetone and absolute ethyl alcohol required repeated applications of fluid. Indentations were made successively at 1.0 mm intervals to produce a rectangular grid.

Upon conclusion of indenting the fluid was removed, using the micropipet, and the diagonals measured. Vicker's hardness was calculated as

$$H = 1854.4\ P/d^2$$

where

P = loads in grams

d = length of diagonal in μ meters

For each fluid tested, a total of 90 tests were made--10 at each of 15, 100 and 1000 grams for loading periods of 5, 15 and 30 secs. An average of the

10 tests for each combination of load and loading period was determined for each fluid. The Vickers hardness (kg/mm^2), standard deviation, load, and type of fluid is shown in Tables III and IV. As can be seen, the Vickers hardness is lowest for ethanol and varies with the load used in the test. These data of hardness are plotted versus dielectric constant of the fluid in Figs. 10 and 11. At high loads the variation in hardness is less than at light loads. This type of result had previously been reported by Cuthrell in drilling experiments of glass. As can be seen, there was not a large difference between the Vickers hardness values for the (100) and (111) surfaces. These results are interpreted as follows: at light loads, adsorption of fluids influences the surface plasticity by affecting the dislocation mobility. The dielectric constant is significant since this parameter relates to the strength of adsorption and the depth of the Debye layer in the fluid. The Debye layer is described by

$$K \propto \left(C_i Z_i^2\right)^{\frac{1}{2}}$$

where both the ionic concentration C_i and valence of the ions Z_i in solution influence the length. At high loads, stresses cause cracking at the perimeter of the pyramid indentation and this overwhelms the adsorption phenomenon.

3.5 Effect of Fluid on the Fracture Strength of Silicon

Silicon wafers were abraded in the presence of fluids then fractured in air at room temperature by a three point bend apparatus. The strain rate was chosen as 0.1 in/min. and a 20 lb full scale load cell was used. The abraded linear groove simulated a thumbnail crack which was produced with a dead loaded diamond. The depth of the groove was controlled by the number of linear traverses of the diamond. Some preliminary results of

ORIGINAL PAGE IS
OF POOR QUALITY

bending stress versus the (groove area)$^{\frac{1}{2}}$ is shown in Fig. 12. As expected, the bending stress decreases as the depth of the groove increases. In addition, the strength for the silicon abraded in the presence of ethanol is lowest while that for water is highest. These results are consistent with the fact that the grooves generated in ethanol are the largest. In addition, the plasticity at the bottom of the groove will also affect the bending strength. The size of this plastic zone can be determined by calculating the difference in bending strength, given the flaw depth, and the experimentally determined stress.

In addition to the bending stress, the morphology of the fracture surface of the silicon can provide important clues to the fracture mechanism.

The morphology of the fracture surfaces of brittle materials is characterized by mirror, mist and hackle regions. For the case of glass [16], the radius of the mirror and the strength are related by

$$\sigma_F r_M^{\frac{1}{2}} = A$$

where σ_F is the fracture strength and r_M is the radius of the mirror region.

A similar relation has been developed by Griffith-Orowan-Irwin where the mirror radius is related to the flaw size by

$$\sigma a^{\frac{1}{2}} = Y\sqrt{EY}$$

where σ is the applied stress, a the flaw depth, Y a geometric constant, E the elastic modulus and γ the surface energy. At the critical load $\sigma = \sigma_c$ and $\gamma = \gamma_c$. The fracture energies can be calculated from the proportionality constant A and flaw-to-mirror size ratio.

Some preliminary data on fracture surface morphology of germanium fracture surfaces has been obtained. Figure 14 shows a SEM of a germanium surface, the germanium was fractured after a groove was abraded in ethanol. The micrograph shows the groove, mirror and hackle regions. The flaw to mirror size ratio is obtained as 0.25. Experiments on silicon surfaces are being carried out.

4. CONCLUSIONS

The conclusions of this first year may be summarized as follows:

a. The abrasion of silicon by diamond is influenced by the fluid in contact with the silicon. Ethanol appears to result in the greatest wear rate while de-ionized water with additions of NaCl appears to result in the lowest wear rate.

b. The mechanism of wear depends on the fluid. The silicon surface abraded in ethanol appears to be less brittle than when abraded in the other fluids.

c. A lateral crack model is more appropriate for the ethanol abraded surfaces while a brittle fracture model is appropriate for the other fluids.

d. The depth of damage as exhibited by subsurface cracks at the bottom of the abrasion grooves depends on the fluid used in abrasion.

e. Microhardness tests of silicon in eight fluids shows that the microhardness is a strong function of load and the dielectric constant ε of the fluid. A maximum of 25% decrease in hardness was observed between water and ethanol.

f. The bending strength of silicon is influenced by the fluid used to abrade a thumbnail crack prior to testing.

REFERENCES

1. Low Cost Solar Array Project, Project Rep. 16, DOE/JPL-1012-51, September 1980 (U.S. Department of Energy - Jet Propulsion Laboratory).

2. Silicon Device Processing, NBS Special Publication 337, U.S. Department of Commerce, November 1970.

3. P. A. Rehbinder, Proc. Sixth Phys. Conf., State Press, Moscow (1928) 29; Z. Phys. 72 (1931) 91.

4. P. A. Rehbinder and E. D. Schukin, Prog. Surf. Sci. 3(2) (1972) 97; A. R. C. Westwood, J. S. Ahearn and J. J. Mills, Colloids and Surfaces, 2 (1981) 1; A. R. C. Westwood and F. E. Lockwood in Microscopic Aspects of Adhesion and Lubrication, Proc. 34th Int. Mtg. of Soc. Chimie Physique, Elsevier (1982), in press.

5. N. H. Macmillan in Proc NATO Advanced Study Institute on Surface Effects in Crystal Plasticity, Hohegeiss, September 5-14, 1975, Noordhoff, Leiden (1977) 629.

6. B. M. Berry in Integrated Silicon Device Technology Vol. XII Measurement Techniques, Publ. Research Triangel Institute, September 1966, p. 135.

7. S. Danyluk and R. Reaves, Wear, 77 (1982) 81-87.

8. E. Rabinowicz, L. A. Dunn and P. G. Russel, Wear, 4 (1961) 345. E. Rabinowicz, Friction and Wear of Materials, Wiley, New York, 1965.

9. A. G. Evans in The Science of Ceramic Machining and Surface Finishing II, NBS Special Publication, 562, U.S. Department of Commerce (1979) 1.

10. J. T. Hagan, J. Mater. Sci. 14 (1979) 2975-2980.

11. C. P. Chen and M. Leipold, Amer. Cer. Soc. Bull. 59 (4) (1980) 469-472.

12. See, for example, Proc. NATO Advanced Study Institute on Surface Effects in Crystal Plasticity, Hohegeiss, September 5-14, 1975, Noordhoff, Leiden (1977).

13. R. E. Cuthrell, J. Appl. Phys., 49 (1978) 432.

14. CRC Handbook, 60th Edition, CRC Press (1980).

15. J. O'M. Bockris and R. K. Sen, Surf. Sci., 30 (1972) 237.

16. J. J. Mecholsky, R. W. Rice and S. W. Freiman, J. Amer. Cer. Soc., 57 (1974) 440.

Table I

Changes of Surface Hardness of Silicon

Reference	Effect	Percent Softening	Comments
Kuczynski and Hochman	Photon irradiation	70% softening	Intensity and surface preparation important; microhardness test
Ablova	H_2O adsorption	Softening	Surface preparation and impurity content important; microhardness test
Westbrook and Gilman	Potential between indenter and crystal	60% softening	Disappeared at elevated temperatures; microhardness test
Yost and Williams	NaCl and $Na_4P_2O_7$	50-80% softening depending on concentration	Zeta-potential measurements of crushed silicon
Cuthrell	CCl_4 and H_2O adsorption	Not determined	Adsorption changed mode of drilling
This work	H_2O, ethanol, acetone adsorption	Up to 70% softening dependent on type of fluid and F_N	Pyramid diamond scratch test

Table II

The Slope dA/dt (Abraded Area Versus Time) of the Experimental Results from Fig. 6 and Eqs. (1) and (3) for (100) n-type Silicon.

Fluid	$\frac{dA}{dt}$ ($x10^{-13}$ m^2/s) Rabinowicz Model Eq. (1)	$\frac{dA}{dt}$ ($x10^{-13}$ m^2/s) Evans Model Eq. (3)	$\frac{dA}{dt}$ ($x10^{-13}$ m^2/s) Experimental data of Fig. 6
De-ionized water	1.0	70.5	1.8
5 w/o NaCl + de-ionized water	0.9	68.8	3.5
Acetone	1.2	77.6	1.9
Ethanol	1.5	87.4	21

Table III

Vickers Hardness for (100) n-Type Silicon

Fluid	Vickers Hardness kg/mm^2	Standard Deviation	Load (gm)
5% - NaCl	1845	298	15
	1756	175	25
	1461	57	50
	1232	77	100
	922	25	1000
De-ionized Water	1842	241	15
	1753	191	25
	1409	43	50
	1255	26	100
	909	16	1000
Toluene	1867	177	15
	1586	177	25
	1329	3	50
	1206	25	100
	934	18	1000
Acetone	1694	169	15
	1549	59	25
	1362	63	50
	1224	56	100
	918	54	1000
Ethanol	1374	176	15
	1302	105	25
	1301	70	50
	1120	82	100
	881	26	1000

Table IV

Vickers Hardness for (111) p-Type Silicon

Fluid	Vickers Hardness kg/mm^2	Standard Deviation	Load (gm)
5% - NaCl	2193	371	15
	1657	108	25
	1448	65	50
	1347	99	100
	981	45	1000
De-ionized Water	1958	108	15
	1299	77	100
	949	53	1000
Toluene	1911	163	15
	1742	143	25
	1419	125	50
	1268	89	100
	924	33	1000
Acetone	1659	123	15
	1506	117	25
	1419	97	50
	1185	53	100
	886	28	1000
Ethanol	1294	217	15
	1073	54	100
	898	47	1000
Methanol	1467	119	15
	1156	46	100
	911	31	1000
50% Methanol-50% Ethanol	1542	116	15
	1102	51	100
	917	50	1000
Glycerol	--	--	15
	1223	53	100
	901	28	1000

Influence of Fluids on the Surface
Mechanical Properties of Semiconductors

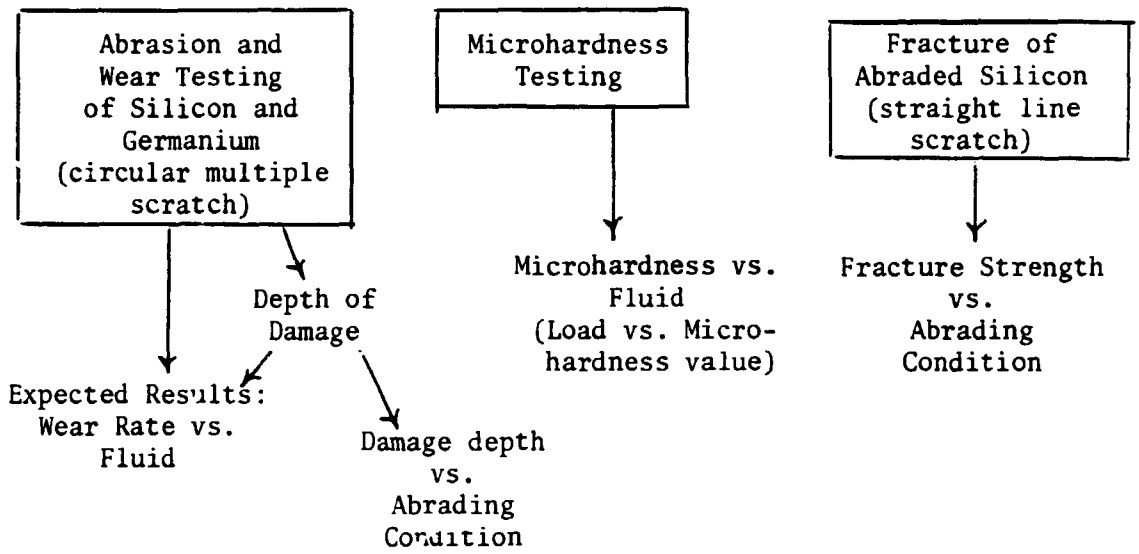

Fig. 1 Flowchart of the experimental program.

ORIGINAL PAGE IS
OF POOR QUALITY

Fig. 2 Schematic diagram of the experimental arrangement. The inset shows the semiconductor which is rotated at 0.56 rps past a stationary 110° conical diamond. The schematic shows median and lateral cracks and conchoidal fractures at the side walls of the generated groove. The normal force F_N and fluid in contact with the semiconductor are varied.

PRECEDING PAGE BLANK NOT FILMED

ORIGINAL PAGE IS
OF POOR QUALITY

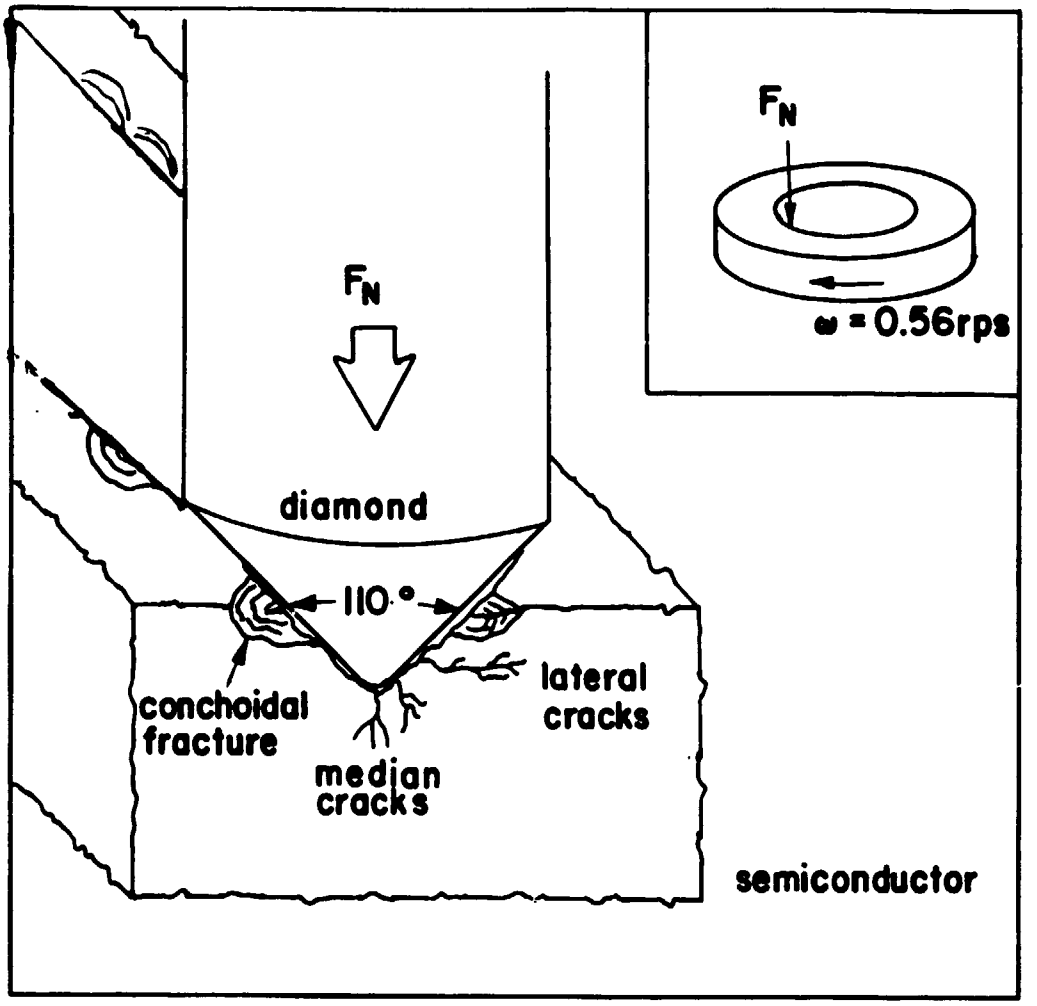

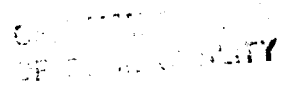

Fig. 3 SEM micrographs of silicon abraded at room temperature by a 110° conical diamond in the presence of (1) de-ionized water, (2) ethanol, (3) acetone and (4) 5% NaCl + de-ionized water. The normal force was 10 gf and the abrasion time was 1.8×10^3 s, all other conditions being held constant.

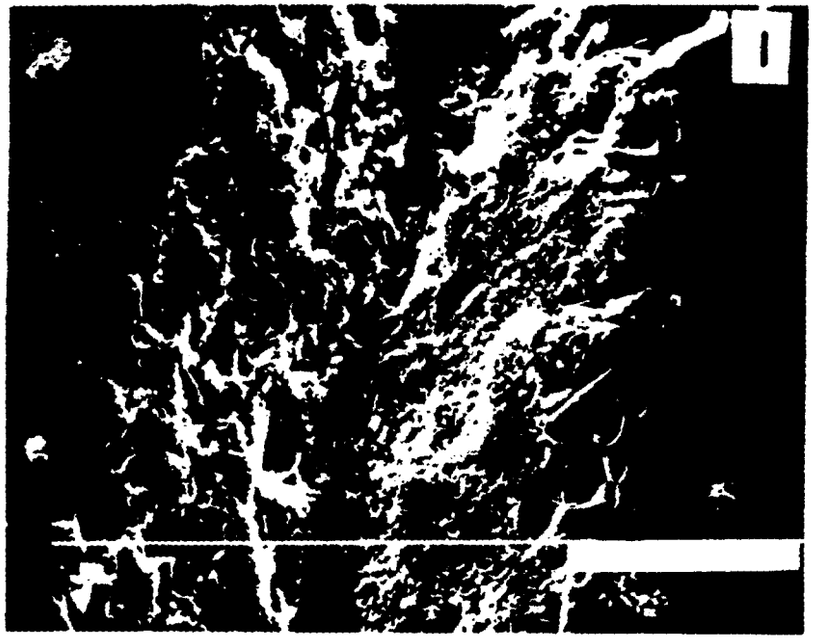
1

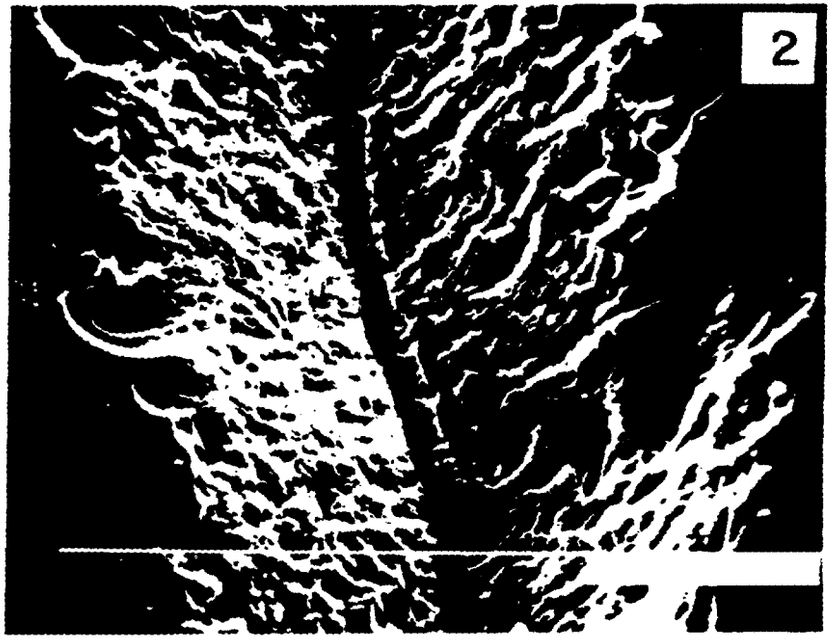
2

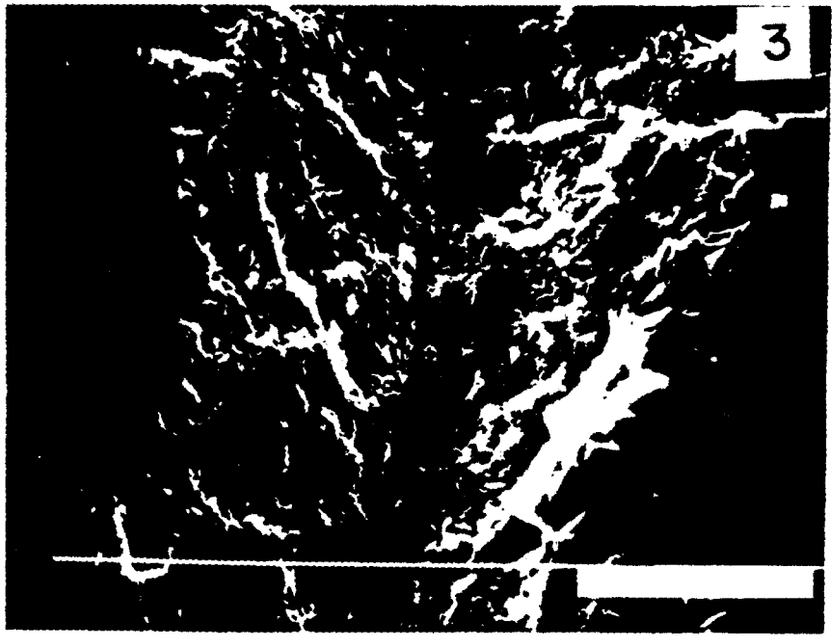
3

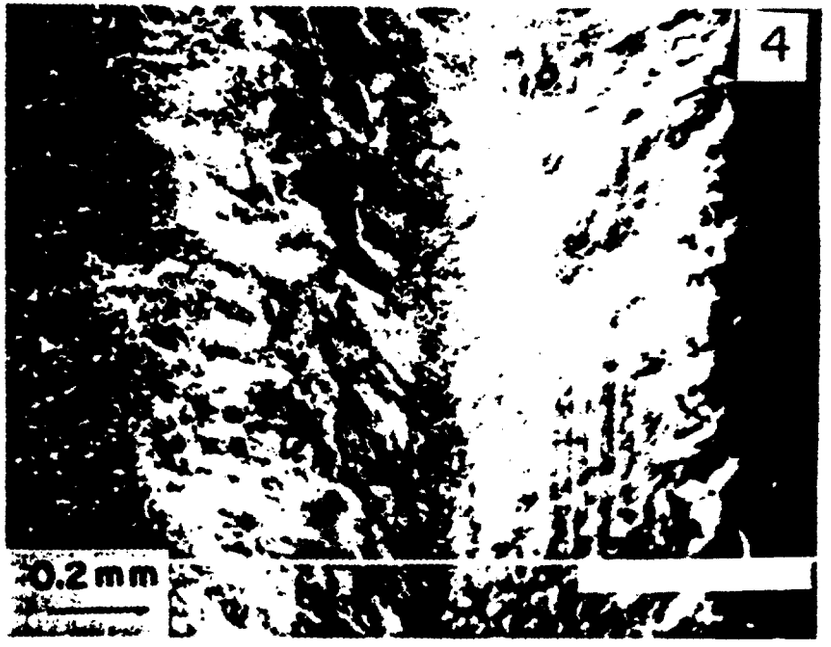
4
0.2 mm

ORIGINAL PAGE IS
OF POOR QUALITY

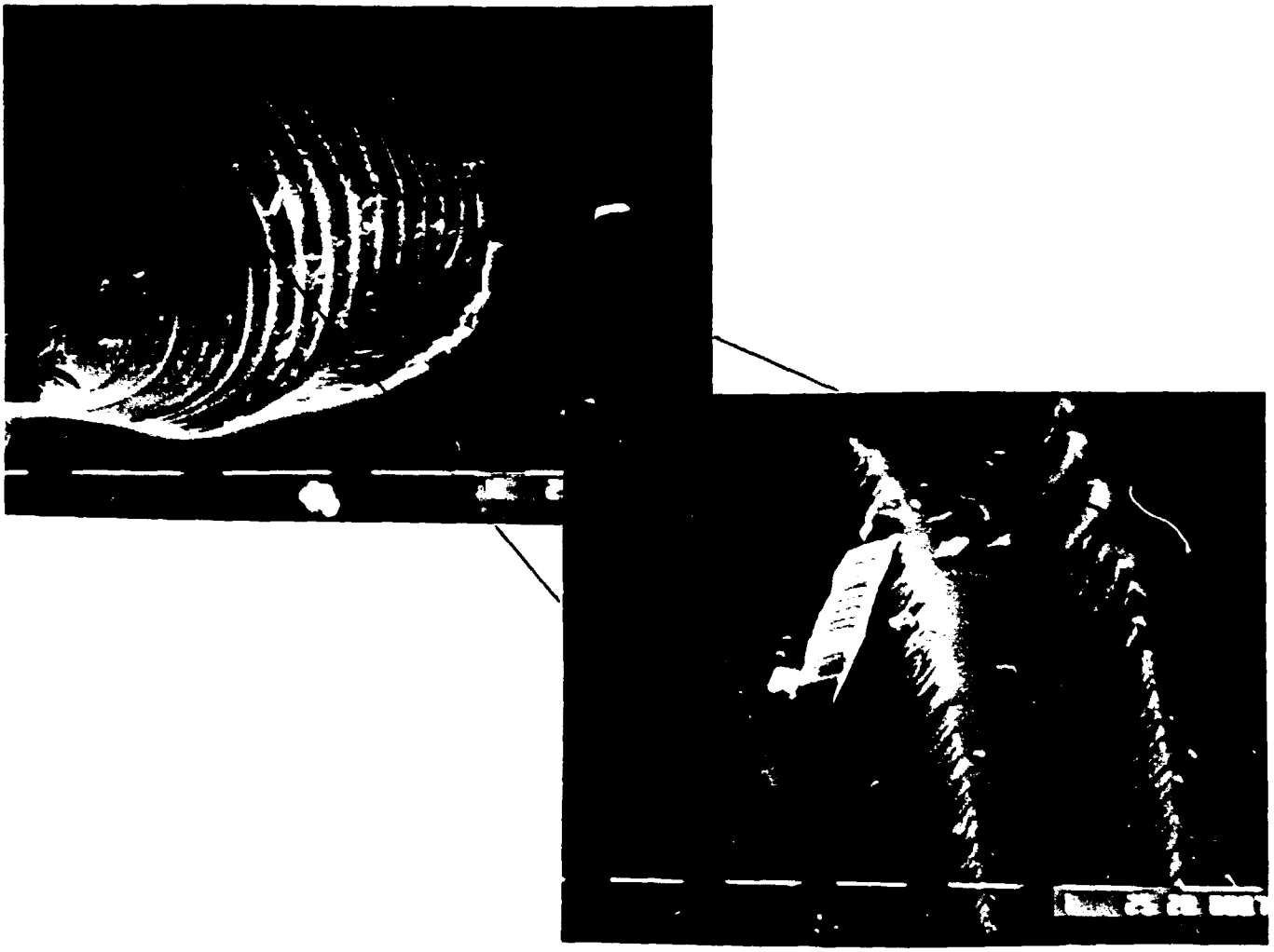

Fig. 4 Scanning electron micrographs of a conchoidal fracture typically seen. A terraced structure is visible along with debris particles.

C...
OF P...

Fig. 5 The abraded cross-sectional area ($x10^{-3}$ mm^2) of the groove of (100) n-type silicon formed by a 110° conical diamond at room temperature versus abrasion time (s) for the four fluids. The normal force F_N was 5 gf.

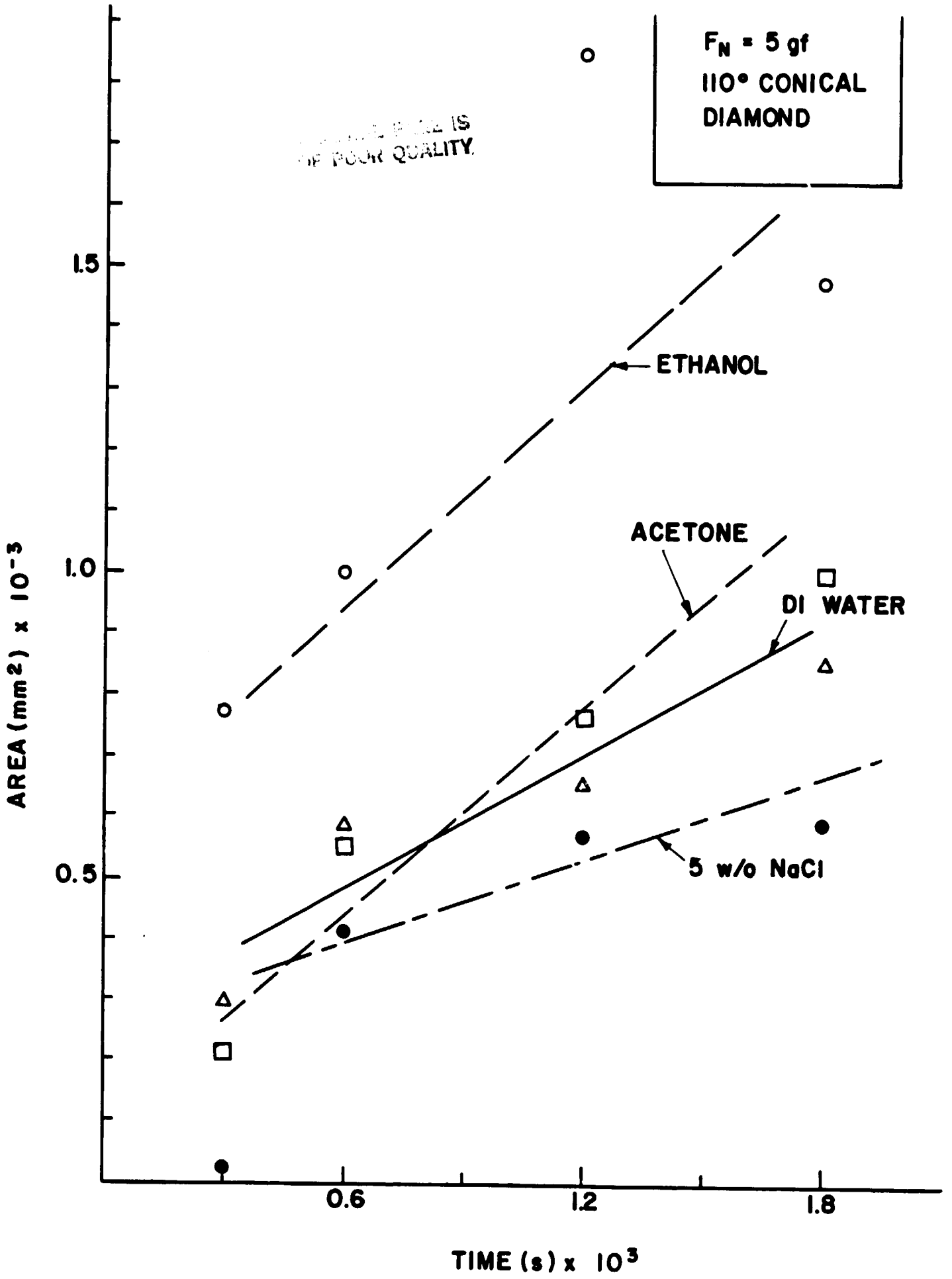
F_N = 5 gf
110° CONICAL
DIAMOND
ETHANOL
ACETONE
DI WATER
5 w/o NaCl
AREA (mm²) x 10⁻³
TIME (s) x 10³
0.5
1.0
1.5
0.6
1.2
1.8

ORIGINAL PAGE IS
OF POOR QUALITY

Fig. 6 The abraded cross-sectional area ($x10^{-3}$ mm^2) of the groove of (100) n-type silicon formed by a 110° conical diamond at room temperature versus abrasion time (s) for the four fluids. The normal force F_N was 10 gf.

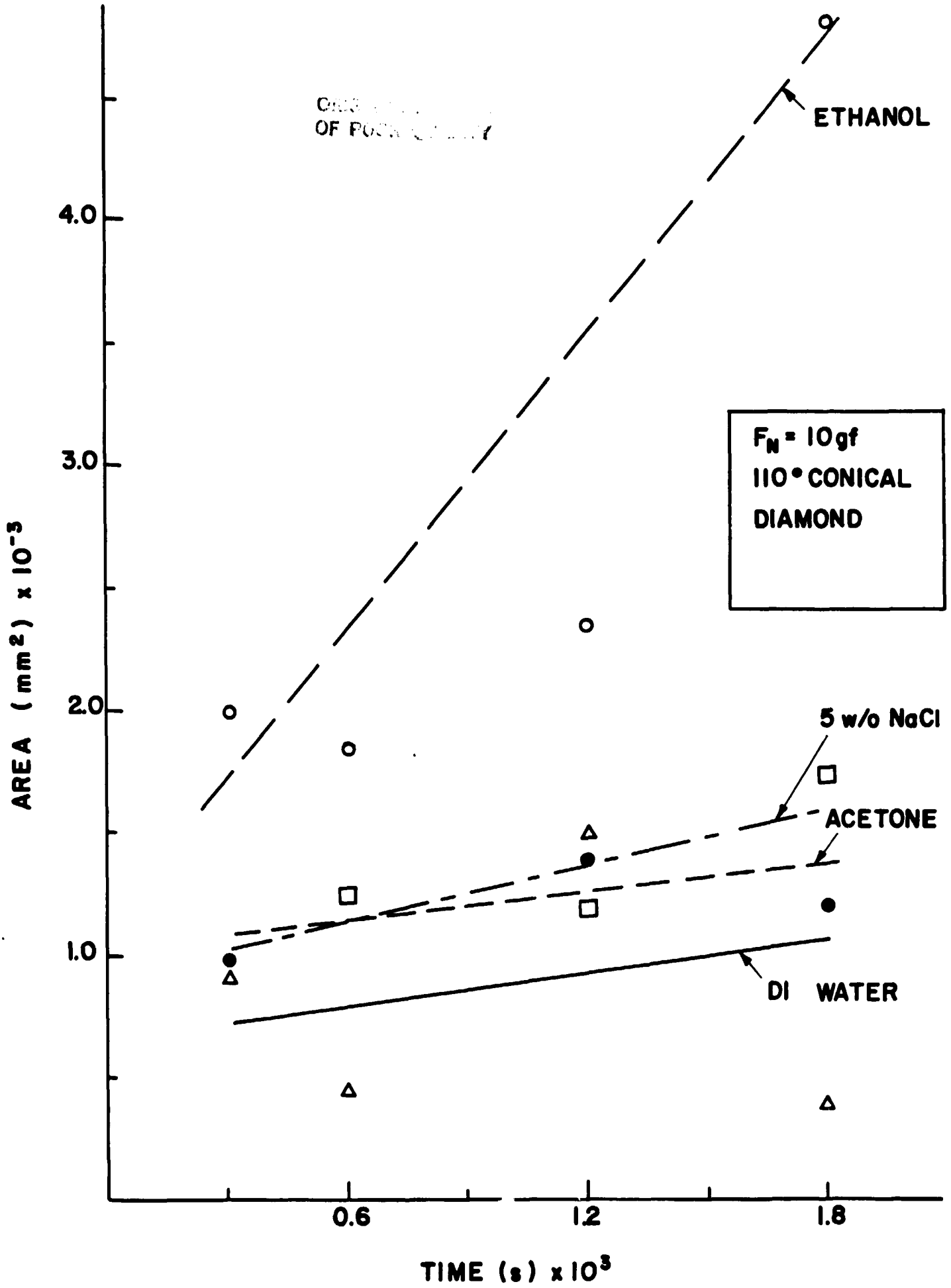
ETHANOL
F_N = 10gf
110° CONICAL
DIAMOND
5 w/o NaCl
ACETONE
DI WATER
AREA (mm²) x 10⁻³
4.0
3.0
2.0
1.0
0.6
1.2
1.8
TIME (s) x 10³

Fig. 7 Schematic diagram of the 5° polishing jig before and after lapping and polishing. The inset shows the geometry of the polished and etched surface. The measured area and subsurface cracks are indicated.

OF POOR QUALITY

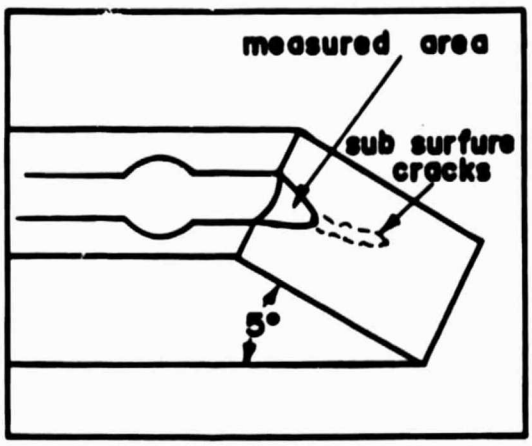

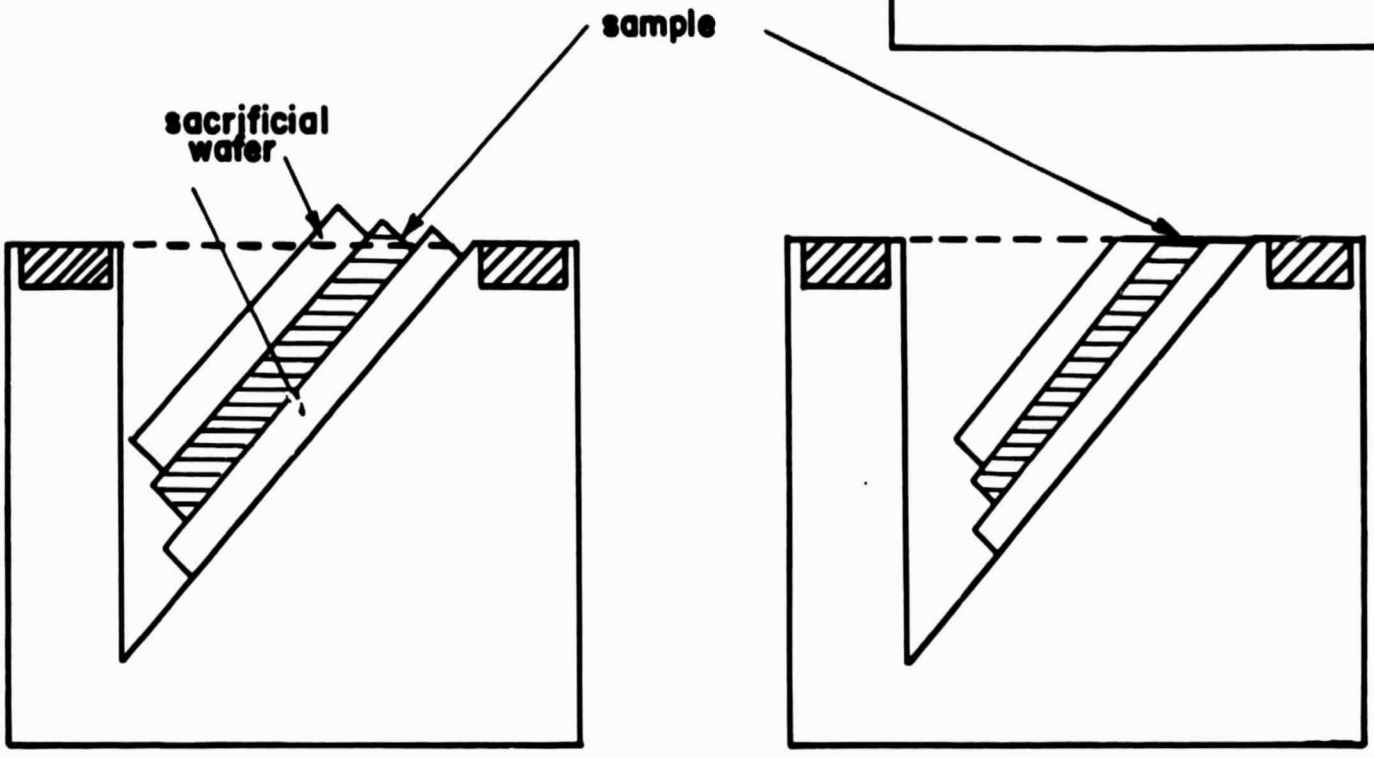

BEFORE LAPPING AND POLISHING

AFTER LAPPING AND POLISHING

Fig. 8 Optical micrographs of 5° bevel polished and etched (100) silicon wafers. The groove depth varies with abrasion time and fluid, with ethanol resulting in the deepest depth of damage. In addition, subsurface cracks are seen below the bottom edge of the groove. F_N = 5 gf.

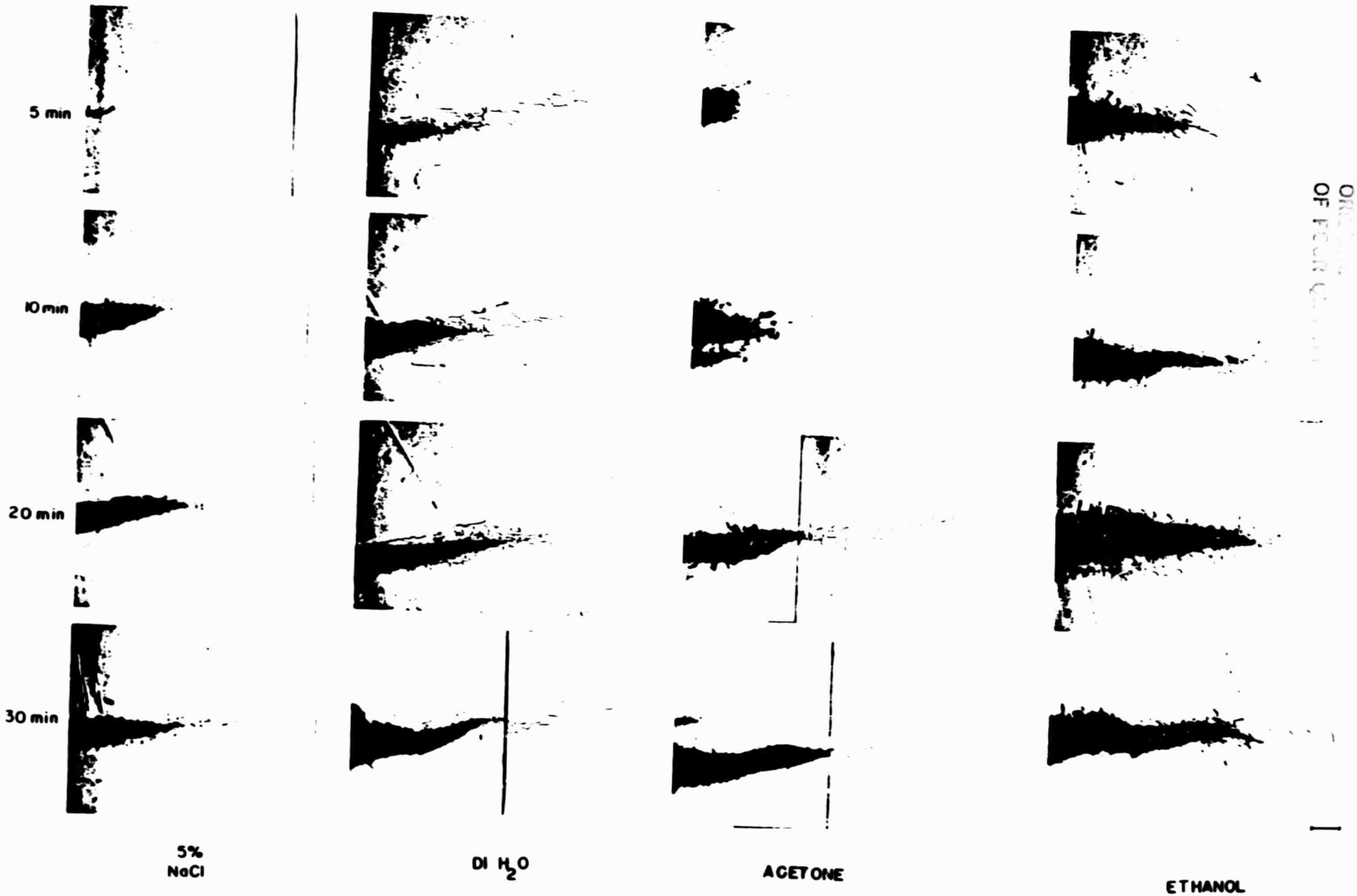
5 min
10 min
20 min
30 min
5% NaCl
DI H_2O
ACETONE
ETHANOL

OF POOR QUALITY

Fig. 9 Abraded area (mm^2) of the 5° polished and etched groove in (100) n-type silicon versus abrading time. The normal force F_N = 5 gf and the fluids are indicated.

ORIGINAL PAGE IS
OF POOR QUALITY

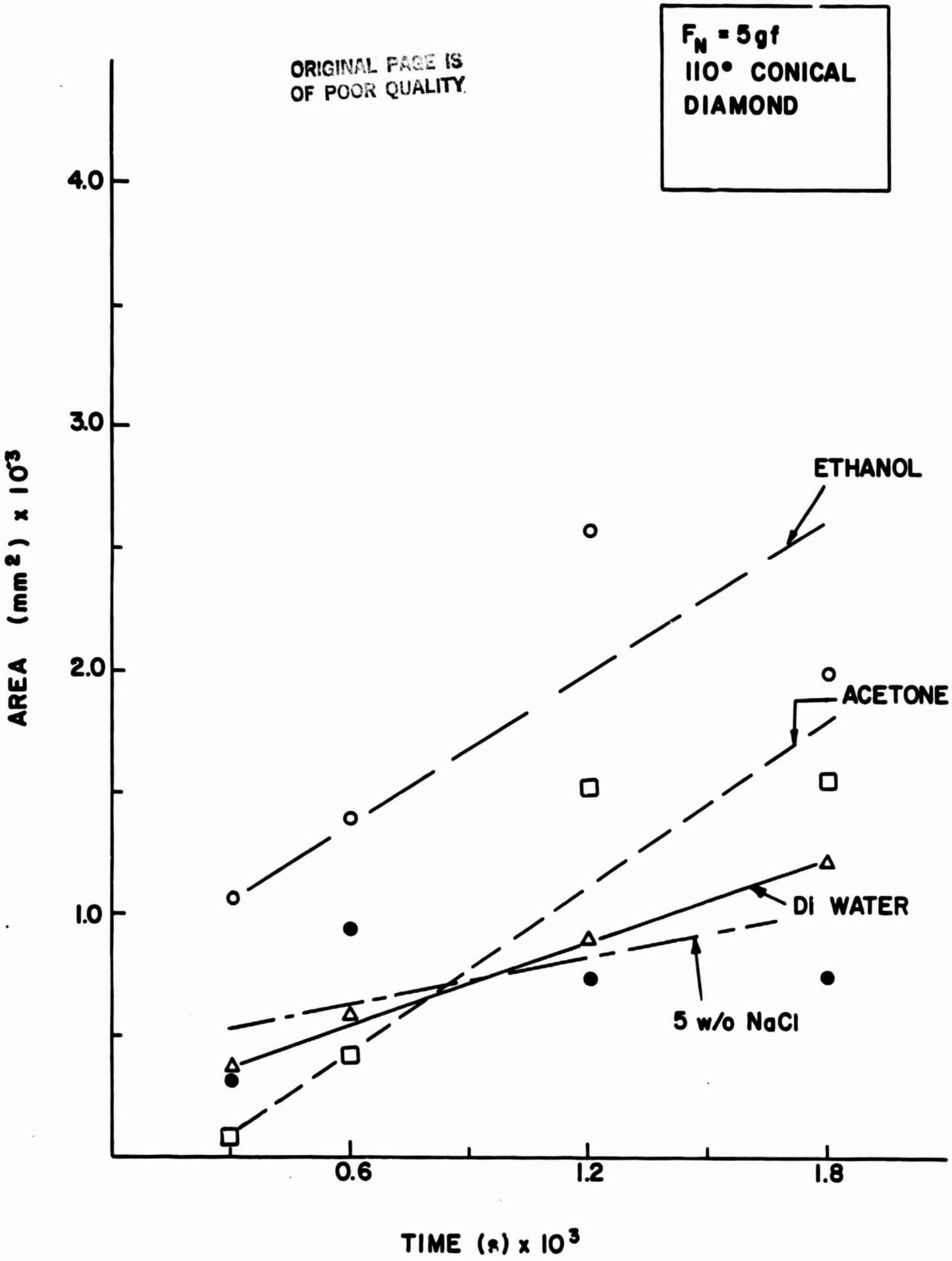

Fig. 10 Vickers hardness (kg/mm^2) versus the dielectric constant of the fluid in contact with the (100) silicon surface.

ORIGINAL PAGE IS
OF POOR QUALITY

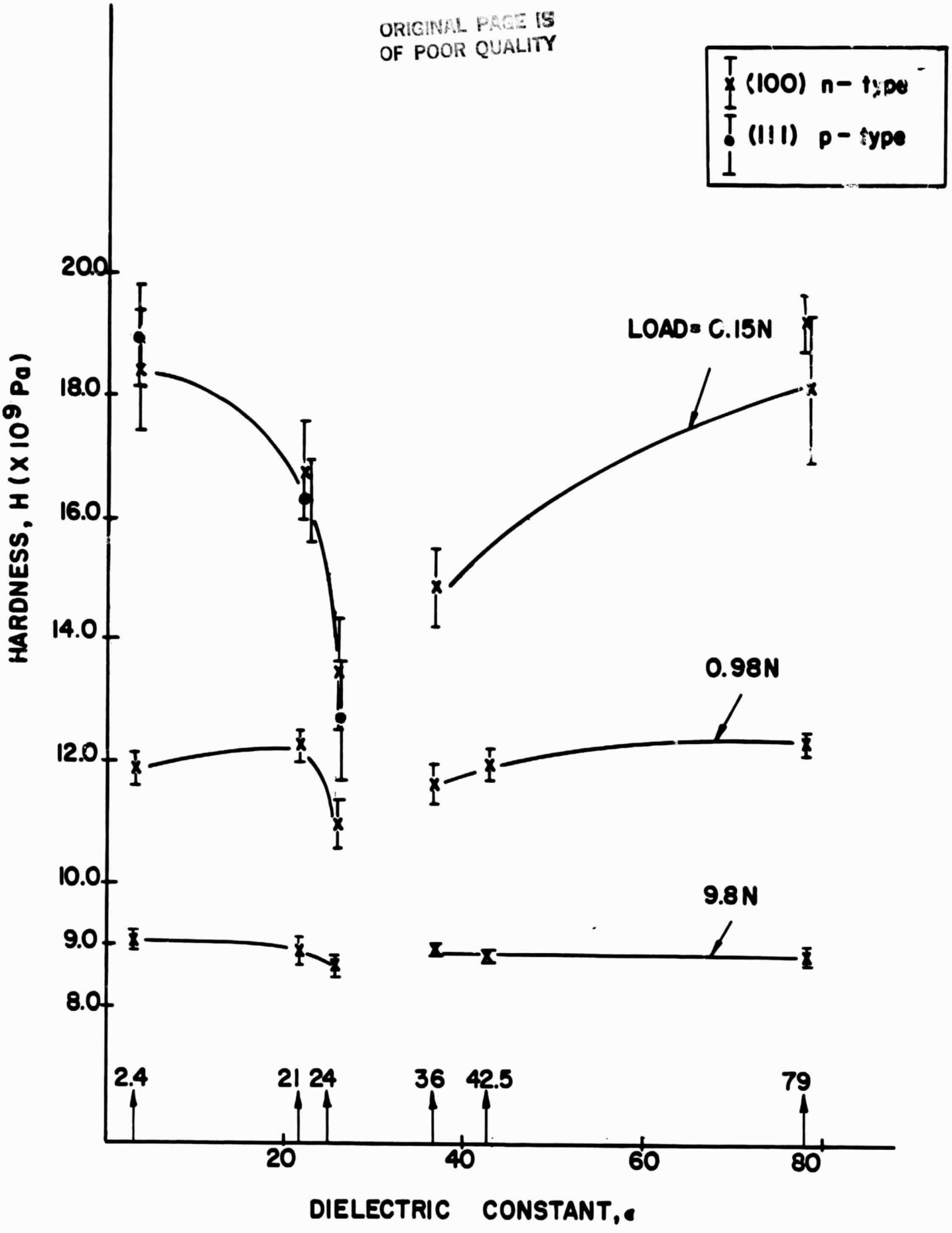

Fig. 11 Vickers hardness (kg/mm^2) versus the dielectric constant of the fluid in contact with the (111) silicon surface.

ORIGINAL PAGE IS
OF POOR QUALITY

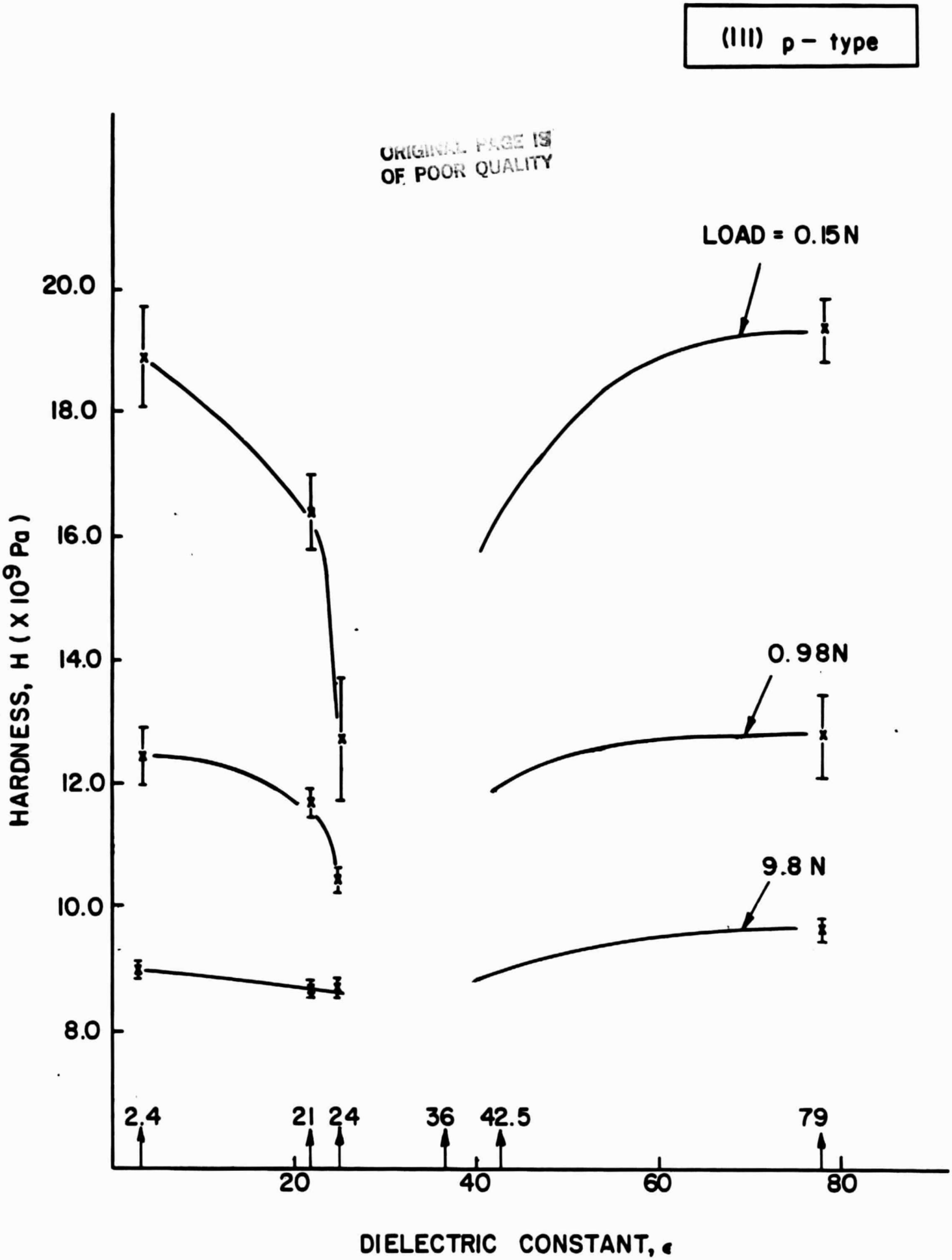

Fig. 12 Bending stress to fracture versus the number of scratches, equivalent to the depth of the groove formed.

ORIGINAL PAGE IS
OF POOR QUALITY

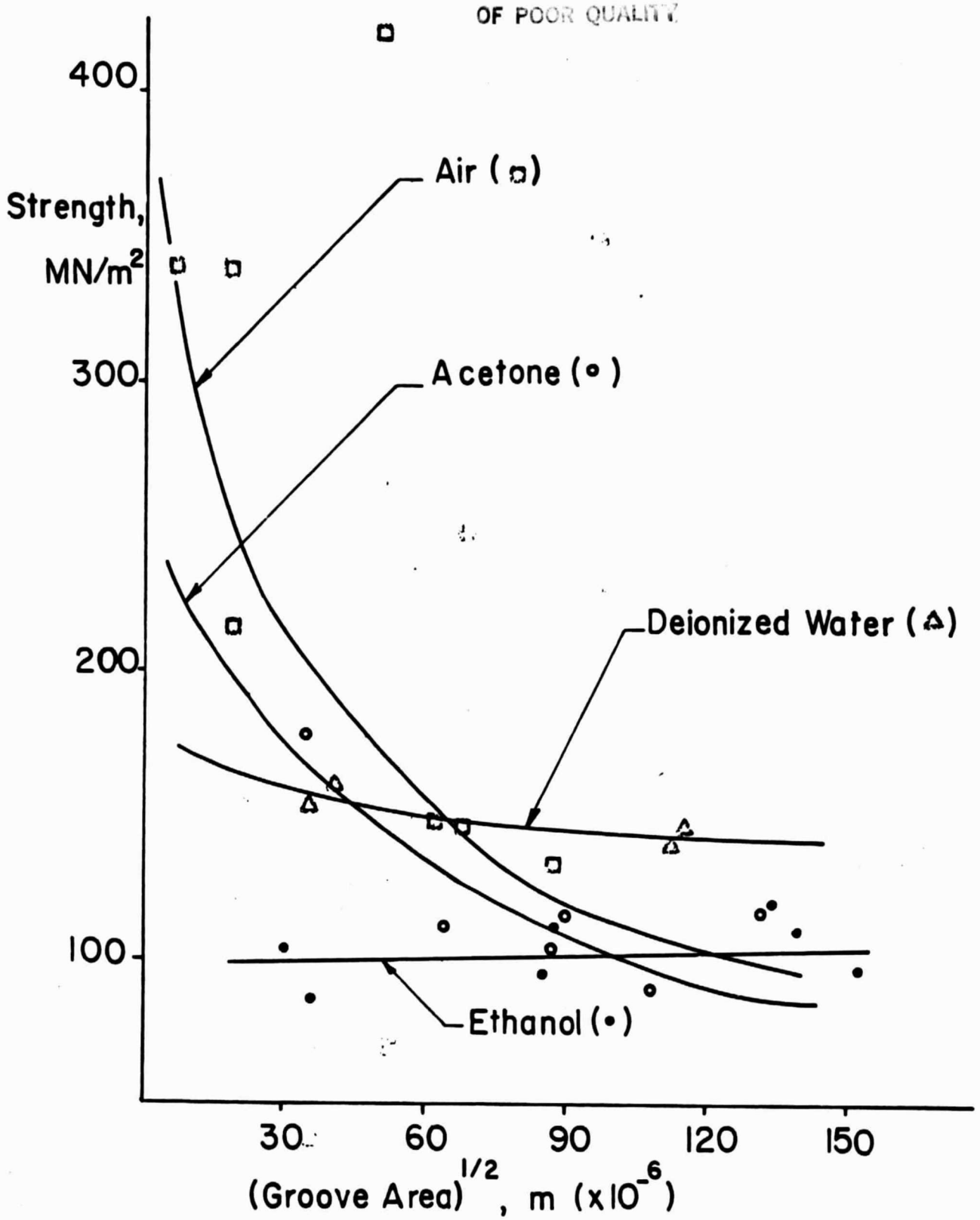

ORIGINAL PAGE IS
OF POOR QUALITY

Fig. 13 A SEM of the fracture surface of germanium. The groove was formed in an ethanol environment with F_N = 20 gf.